Branching and angular distribution of photofragments in two-frequency intense-field multiphoton dissociation of HD^+

Bibhas Dutta, Sanjay Sen, Samir Saha, and S. S. Bhattacharyya*

Atomic and Molecular Physics Section, Department of Materials Science, Indian Association for the Cultivation of Science, Jadavpur, Kolkata 700 032, India

(Received 9 October 2002; revised manuscript received 6 March 2003; published 2 July 2003)

We have investigated the branching ratios and angular distributions of photofragments resulting from the two-frequency multiphoton dissociation of HD^+ from initial bound level $v_i=0, J_i=0$ induced by linearly polarized parallel laser fields of equal intensity of 1 TW/cm^2. Both the laser frequencies ω_1 and ω_2 are below the dissociation threshold with $\omega_1<\omega_2$. We have used the time-independent close-coupling method. Molecular rotation has been taken into account with $J=0-9$ in each of the two electronic states GS and ES. The photon absorption channels (n_1,n_2) with $n_1,n_2=0-3$ have been included when n_1 and n_2 are the numbers of photons of frequencies ω_1 and ω_2 absorbed. We have neglected absorption channels when (net) four or more photons are involved. This necessitates the use of 120 channels. All radiative couplings including those due to the intrinsic dipole moments of HD^+ have been considered in a truncated length gauge form of interaction. In the presence of intermediate photon vibrational resonance with the GS (1,0) channel, dissociation takes place mainly through the ES (1,1) channel. But the channel ES (1,2) dominates for frequency ω_2 not satisfying the resonance condition. For linear polarization, preferential photofragment ejection along the field polarization direction (i.e., $\theta=0°$ or 180°) takes place. On resonance, the angular distribution shows prominent rings that are peaks on the photofragment distribution away from $\theta=0°$. We have presented the photofragment angular distributions of HD^+ for different (open) photon channels within the framework of dressed state picture, vibrational trapping and the bond softening, adiabatic path, and the nonadiabatic transition mechanisms.

DOI: 10.1103/PhysRevA.68.013401 PACS number(s): 42.50.Hz, 33.80.−b

I. INTRODUCTION

The multiphoton excitation schemes of molecules with discrete multifrequency fields have currently generated a lot of interest both as a mechanism of controlling molecular processes and as a means of understanding the basic physics behind such processes occurring in presence of intense laser fields. The multifrequency excitation schemes studied theoretically and experimentally can be basically divided into two types. In the first type the fields are coherent with stable phase relations between them and the frequencies are generally multiples of one another. The interference between amplitudes of the different paths from the initial to a final state depends on the field characteristics, which are often used to steer the dynamics of a process on a specific course, such as by changing the relative phases of the fields. On the other hand, two or more lasers with no particular phase relation between them have often been used to explore different aspects of the laser induced states of an atomic or molecular system. These states arise due to the very considerable distortion or dressing that such a system undergoes in the presence of intense fields. These dressed states due to an intense laser field can most conveniently be investigated by using another weak probe field. Such pump-probe interactions have been also explored for many systems for gaining information about the modifications created by the laser in an atomic or molecular system. Theoretically, a perturbative treatment of the pump field is inapplicable and a perturbation theory for the probe field is reformulated in the basis of the new dressed states obtained by the action of the pump field. Specifically, in the molecular context, we may say that the field dressing of the molecule by the pump field implies distortion of the electronic charge cloud around the nuclear framework, and produces modification of the molecular potential-energy surfaces on which the nuclei move. In a pump-probe situation, the transition from one such modified potential surface to another is envisaged.

However, this pump-probe picture cannot be applied when two fields of equal intensities interact with a molecular system. Both the fields can cause drastic modifications of the potential surface and the resulting motion of the molecule can be very complicated indeed. The best way to calculate the response of a molecular system is to treat the interaction of these two fields with the molecule on an equal footing. The two fields, acting simultaneously, may modify the transition frequencies, transition widths, and the fragmentation pattern of the molecule in ways which are not intuitively obvious and which cannot be estimated without detailed numerical computation.

The simplest one-electron molecule H_2^+ and its isotopic analog HD^+ have played key role in the investigation of the effect of strong fields on molecular dynamics because of their simplicity and their well-known electronic structure. Most of the works on these molecules were concerned with their dissociation in a single-frequency field [1–3] or in a bichromatic laser field with two harmonic frequencies bearing a definite phase relation [4,5]. The two molecules have identical electronic structure but because of its heteronuclearity, the isotopic substituent HD^+ has a strong asymptotically diverging intrinsic dipole moment. Also, its transition dipole moment between the lowest electronic states is very

*Email address: msssb@mahendra.iacs.res.in

 ©2003 The American Physical Society

different from that of H_2^+. The presence of the intrinsic dipole moment can cause vibrational-rotational virtual transitions within the ground electronic state by photon absorption or emission. These virtual radiative transitions do have important effects on the branching ratios and widths of the multiphoton dissociative transitions. Apart from this, these vibrational-rotational levels can act as intermediate resonant levels. The characteristics of these intermediate resonances will be strongly dependent on both the intense fields present for suitable frequencies of these fields.

In a previous paper [6], it was shown in a crude fashion how these intermediate levels play a very interesting and significant role in determining the spectrum of the dissociation linewidth in a two-frequency field when both fields have similar intensities. It was also shown that the dressing of the potential curves by the two monochromatic fields causes the appearance of laser induced resonant levels with energies depending on the frequencies of the dressing fields. These laser induced resonances were shown to cause both sharp enhancements and deenhancements in the multiphoton dissociation cross sections as the frequencies are changed. However, the interesting feature was the appearance of multiple resonance peaks in the dissociation linewidth when the nonresonant frequency was varied around the dissociation threshold. In between these peaks the dissociation linewidth almost vanishes. These features were explained as being due to the formation of a set of closely spaced resonance levels by the laser fields in the region where only an isolated resonant level of the free molecule existed. This modification of the energy level structure was due to the distortion of the molecular potential-energy surfaces by the laser fields. The results were obtained by using a one-dimensional model in the time-independent close-coupling (CC) formulation with a limited basis set. Apart from the fact that the molecular dynamics may become qualitatively different when rotations are included, these limitations did not allow the authors [6] to investigate two important observable characteristics of the multiphoton dissociation process. These are the branching ratios of the dissociation fragments to different photon absorption channels and the angular distribution of these fragments in different channels with respect to the direction of the linear polarization of the light fields.

In the present work, we again address the question of the resonant multiphoton dissociation linewidth of HD^+ by two strong linearly polarized fields in the same direction and of equal intensity of 1 TW/cm^2. Now the emphasis is on the branching ratios and the photofragment angular distribution. We show that as the combination of frequencies reaches that required for an intermediate resonance, the branching ratios and the angular distribution undergo drastic changes. In particular, the angular distribution patterns on resonances are radically different from the usual above-threshold dissociation (ATD) patterns investigated earlier [7], which are also obtained in the present two-frequency below threshold case when no intermediate laser induced resonance takes part in the dissociation process.

As in our earlier works [3,6,7], we have adopted the time-independent CC formulation [8]. For this time-independent approach to be valid, the intensities should not vary significantly on the time scale of the fragmentation process and there should be a sufficient number of field cycles within the rise time of the pulse which, in turn, should occupy a length of time substantially less than the time for which the intensity remains essentially constant.

The paper is organized as follows. The following section of the paper will provide the theoretical framework necessary to describe the strong field dissociation process. Section III presents the way the calculations have been made and the values of the different parameters considered. Section IV describes the results and their theoretical explanation. Section V deals with the conclusion.

II. FORMULATION

In the CC approach, the multichannel coupled time-independent Schrödinger equation is solved for the field plus molecule system. For a fixed total energy E_T of the system, the equation is given by

$$H\Psi(E_T)=E_T\Psi(E_T). \tag{1}$$

After eliminating the center-of-mass motion, the total Hamiltonian H of the interacting field plus molecular system in the length gauge is

$$H=T_R+H_0+V_{rad}^L, \tag{2}$$

where T_R is the nuclear kinetic-energy operator corresponding to the radial motion of the nuclei with respect to the center of mass (the coordinate of the radial motion is R), H_0 is the Hamiltonian for the rotating molecule (with fixed internuclear separation R) plus the laser fields in the absence of radiative interaction, and V_{rad}^L is the radiative interaction Hamiltonian between the molecule and the radiation fields in the length gauge.

Thus

$$T_R=-\frac{\hbar^2}{2\mu}\frac{\partial^2}{\partial R^2} \tag{3}$$

and

$$H_0=\sum_j \frac{p_j^2}{2m_j}+T_\Theta(R)+V_C(R)+\hbar\omega_1(a_1^+a_1)+\hbar\omega_2(a_2^+a_2). \tag{4}$$

The first term in Eq. (4) represents the kinetic-energy operator for all electrons, the second term gives the rotational kinetic-energy operator for the nuclear motion with the internuclear separation R as a parameter, the third term is the Coulomb interaction energy between the charges, and the last two terms give the energies of the radiation fields. For solving Eq. (1), the total time-independent wave function $\Psi(E_T)$ for a fixed total energy E_T is expanded in terms of the diabatic or the bare molecule plus field channel states $|d\rangle$ which are eigenfunctions of H_0,

$$\Psi_T(N_1,N_2,E_T,R)=\frac{1}{R}\sum_d |d\rangle F_d(R), \tag{5}$$

where $F_d(R)$ are the components of the wave vector **F** of radial nuclear motions in channel states $|d\rangle$ and

$$|d\rangle = |\Lambda, J, n_1, n_2\rangle = \Phi_\Lambda(\mathbf{r}, R) Y_{JM}(\theta, \phi) |N_1 - n_1, N_2 - n_2\rangle. \tag{6}$$

Here Λ denotes the index of electronic state whose wave function is $\Phi_\Lambda(\mathbf{r}, R)$, **r** are the electronic coordinates, and n_1 and n_2 are the numbers of photons of frequency ω_1 and ω_2 absorbed or emitted whose initial numbers were N_1 and N_2, respectively. We have taken $\omega_1 < \omega_2$ and both are below the dissociation threshold. Thus, here $|N_1 - n_1, N_2 - n_2\rangle$ is the photon number state with $N_1 - n_1$ and $N_2 - n_2$ numbers of photons of frequencies ω_1 and ω_2 present. In our case, as only two lowest electronic states have been used, Λ will take the values of GS and ES for HD^+. Since both the concerned electronic states are Σ states, the rotational wave function of the molecule can be represented as $Y_{JM}(\hat{R})$, $\hat{R}$ being the angular coordinates of the vector **R** with respect to the space-fixed system of axes. J is the rotational quantum number of the molecule.

The eigenvalue equation for the unperturbed Hamiltonian H_0 is

$$H^0 |d\rangle = W_d^0(R) |d\rangle \tag{7}$$

with

$$W_d^0 = V_\Lambda(R) + \frac{\hbar^2}{2\mu} \frac{J(J+1)}{R^2} - n_1 \hbar\omega_1 - n_2 \hbar\omega_2 \xrightarrow[R\to\infty]{} E_\Lambda - n_1 \hbar\omega_1 - n_2 \hbar\omega_2. \tag{8}$$

W_d^0 are the eigenvalues of the channel states $|d\rangle$ with the origin shifted by the initial energies of the fields, i.e., by $N_1 \hbar\omega_1 + N_2 \hbar\omega_2$. E_Λ is the asymptotic energy of the electronic state Λ, whose potential energy is given by $V_\Lambda(R)$. The second term of Eq. (8) gives the centrifugal potential energy in the angular-momentum state J. The observable asymptotic kinetic energy of the system is given by

$$\varepsilon_d = E - E_\Lambda + n_1 \hbar\omega_1 + n_2 \hbar\omega_2. \tag{9}$$

For $\varepsilon_d \leqslant 0$ the channel d is closed and for $\varepsilon_d > 0$ it is open. Since the solution does not depend on the origin of the energy scale, all of the energies have been measured with respect to $N_1 \hbar\omega_1 + N_2 \hbar\omega_2$, i.e., the initial field energy and E is the total energy of the system measured from this origin.

Thus, substituting Eq. (5) into the Schrödinger Eq. (1), we obtain the matrix form of the coupled second-order differential equations for the wave functions $F_d(R)$ of the radial nuclear motions at energy E as

$$\left[\frac{\partial^2}{\partial R^2} + \frac{2\mu}{\hbar^2}(E - U) \right] \mathbf{F} = 0, \tag{10}$$

where

$$U_{dd'}(R) = W_d^0(R)\, \delta_{dd'} + V_{dd'}(R)\, \delta_{n_1', n_1 \pm 1} \delta_{n_2', n_2} + V_{dd'}(R)\, \delta_{n_1', n_1} \delta_{n_2', n_2 \pm 1} \tag{11}$$

with [7]

$$V_{dd'}(R) = \langle d' | V_{rad}^L | d \rangle = 1.171 \times 10^{-3} D_{\Lambda'\Lambda}(R) \sqrt{I} \times [(2J'+1)(2J+1)]^{1/2} (-1)^M \begin{pmatrix} J' & 1 & J \\ -M' & 0 & M \end{pmatrix} \times \begin{pmatrix} J' & 1 & J \\ 0 & 0 & 0 \end{pmatrix}. \tag{12}$$

Here $D_{\Lambda'\Lambda}(R)$ is the radial matrix element of the dipole moment operator between the electronic states Λ' and Λ in atomic units, I is the laser intensity in W/cm^2, and the result is in cm^{-1}.

Including a finite number (N_0) of the channel states $|d\rangle$, the coupled equations can be solved for a given E using the standard full-collision boundary conditions on the components of the scattering wave vector **F**. The components of the matrix of the solution, $F_d(E,R)$, of Eq. (10) can give us the required information when the solution is calculated over a large number of total energies. The component of the wave vector, $F_{co}(R)$, corresponding to the closed channel denoted by c, asymptotically goes to zero, while $F_{o'o}$ is described by an incoming wave in the channel o and an outgoing wave in another open channel o' [8]. Thus for each energy E, we obtain an N_0-fold degenerate set of orthogonal energy normalized solutions, by imposing the following asymptotic behavior on the radial wave functions:

$$F_{co}(R) \widetilde{\underset{R\to\infty}{}} 0$$

and

$$F_{o'o}(R) \widetilde{\underset{R\to\infty}{}} \left(\frac{2\mu}{\pi k_{o'} \hbar^2} \right)^{1/2} [e^{-ik_o R} \delta_{o'o} - e^{+ik_{o'} R} S_{o'o}(N,E)]/2iR, \tag{13}$$

where **S** is the $N_0 \times N_0$ unitary scattering matrix.

In the present case, the situation envisaged is a half-collision one, which corresponds to the dissociation of an initial field-free bound state abruptly exposed to strong fields. The full-collision wave functions characterized by **F** can be used to describe the half-collision situation in which an initial field-free bound state i in a particular closed channel c described by χ_{ci} is exposed to the lasers incident at $t = 0$. The wave packet representing the initial state becomes nonstationary, decaying into the complete set of outgoing states and can be expressed as a linear superposition of the time-independent solutions of Eq. (1), which are eigenstates of the total Hamiltonian, as shown by Mies and Giusti-Suzor [8]. Using this picture, the time-independent probability $P_{o \leftarrow i}$ of finding the system in an outgoing wave state o from an initial field-free bound state i in a specific closed channel c with wave function $\chi_{ci}(R)$ can be obtained as

$$P_{o\leftarrow i}(E)=|\langle F^{*}_{co}(E,R)|\chi_{ci}(R)\rangle|^2=|T_{JM}(E,n_1,n_2|i)|^2, \tag{14}$$

where

$$T_{JM}(E,n_1,n_2|i)=\langle F^{*}_{co}(E,R)|\chi_{ci}(R)\rangle. \tag{15}$$

The transition amplitude T is obtained from the solution vector $\mathbf{F}(E,R)$ of the radial equations. The solution for each value of E gives a set of P's for all open channels.

Because of the nonstationary nature of the initial wave packet in the laser fields, a range of energies around the energies of the laser induced states should contribute to this overlap $P_{o\leftarrow i}$. The width of this quantity in the energy scale should give the rate of the decay of the initial wave packet. At moderate intensities, only a single peak is obtained at the same energy for each (open) photon channel. The peaks for all (open) photon channels have the same width, same position, and normally they are almost Lorentzian in shape. This implies that the wave packet undergoes an exponential decay in time and a unique dissociation rate is defined from the width of the peak. The position of the resonance peak on the energy scale defines the dynamic Stark shift of the initial state. It should be stated here that all our present calculations are for the highest (Lorentzian) peak in the photofragment kinetic-energy distribution. There is the possibility of a second lower peak in the fragment kinetic-energy profile at the intermediate and high intensities [6]. It is worth mentioning here that our time-independent CC approach is rigorous and takes into account the presence of higher peaks (resonances) in the kinetic-energy spectrum. Equation (14) properly takes into consideration the higher resonances in the fragment kinetic-energy profile [6]. The total decay probability in a steady field must be unity after a sufficiently long time. Thus the integral of the total overlap

$$T_i(E)=\sum_o P_{o\leftarrow i}(E) \tag{16}$$

over the energy should give unity.

The angular distribution of the photofragments from an initial rovibrational level v_i, J_i is given by Balint-Kurti and Shapiro [9] as

$$P_i(\theta,E_0,n_1,n_2)=k\sum_{JM}|(i)^J Y^{*}_{JM}(\theta,\phi)T_{JM}(E_0,n_1,n_2|i)|^2, \tag{17}$$

where $T_{JM}(E_0,n_1,n_2)$ is the bound-free transition amplitude [Eq. (15)] for n_1 and n_2 photon absorption at peak energy E_0, and θ is the angle between the dissociated fragments and the space-fixed Z axis. The space-fixed Z axis is the direction of the electric-field vector for linearly polarized light. k is some specific constant. It may be noted that P_i is independent of ϕ for axially symmetric molecules.

III. CALCULATIONS

The time-independent close-coupling calculation of the multiphoton dissociation of HD^+ from ground vibrational level in two fields each of intensity 1 TW/cm^2 and frequencies below the dissociation threshold was made by Datta and Bhattacharyya [6], but the effects of different rotational levels were not taken into account by them. However, for appreciation of the complexity of the phenomena and for reliable quantitative estimations it is essential to take rotation into account. In particular, the treatment of the branching ratios and angular distributions of the photofragments resulting from the multiphoton dissociation of HD^+ requires a greatly extended rotational basis set. We have considered molecular rotation by including 120 channels with $J=0$–9. The initial molecular bound level has been taken to be $v_i=0, J_i=0$ and both the laser frequencies ω_1 and ω_2 were chosen below the dissociation threshold with $\omega_1<\omega_2$. ω_1 is so chosen that approximates the energy of the vibrationally excited ac Stark shifted $v=6, J=1$ level with respect to the Stark shifted ground level $v_i=0, J_i=0$. In HD^+, due to mass difference between the nuclei, the g-u symmetry of the two lowest Born-Oppenheimer electronic states $1s\sigma_g$ and $2p\sigma_u$ is broken and the degeneracy of the electronic eigenstates is removed by the nonadiabatic interaction due to the nuclear motion. The two new eigenstates GS and ES arising from the diagonalization of the two coupled g-u states of the Born-Oppenheimer orbitals go asymptotically to the H^+ and $D(1s)$ and $H(1s)$ and D^+ states, respectively, with an energy difference of 29.87 cm^{-1} [10].

The transition dipole moment between the GS and ES states asymptotically goes to zero but the permanent dipole moment increases linearly with R at large R. The nonstandard diverging behavior in the length gauge can be changed by judicious truncation of the interaction. We have included an exponentially decaying cutoff function $e^{-\alpha(R-R_{cut})}$ in the linearly diverging dipole matrix elements beyond $R=R_{cut}$. The value of R_{cut} was adjusted so as to have no effect on the total linewidth. As in our earlier work [3], the value of 20 a.u. for R_{cut} and 0.5 for the exponent α in the decay function were found to be satisfactory because here also the intregation of the CC was continued upto 40 a.u.

The nonadiabatic potentials of the two lowest states GS and ES of HD^+ are obtained from the work of Carrington and Kennedy [11]. The intrinsic electric dipole moments of HD^+ for the GS and ES states are taken from Moss and Sadler [10]. The transition electric dipole moments of HD^+ are calculated from the corresponding Born-Oppenheimer values for transition electric dipole moments of H_2^+, obtained from the works of Bates [12], by the method provided by Ghosh *et al.* [13]. Renormalized Numerov method has been used to obtain the time-independent radial solution vectors by solving the multichannel CC scattering equations. We have properly modified the CC code of Julienne, Mies, and Sando [14] to use in our work.

Henceforth, during discussion, each channel will be labeled by the number of photons absorbed or emitted, i.e., by the notation (n_1,n_2) and either GS or ES depending on whether the electronic state involved is the ground bonding state or upper antibonding state and the total angular momentum J. The channels may be opened or closed depending on the final energy of the field-free molecule. An open photon channel with a positive molecular energy indicates dissocia-

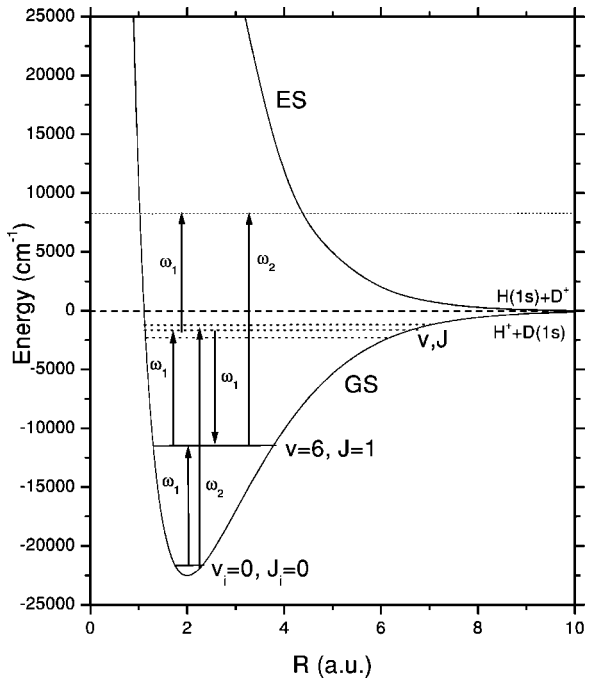

FIG. 1. The two lowest potential-energy curves GS and ES of HD^+ against internuclear separation R. The eigenenergies of the unperturbed bound vibrational-rotational levels $v_i=0,J_i=0$ and $v=6,J=1$ are shown by solid lines. The positions of some other high-lying vibrational-rotational levels near the dissociation threshold have been indicated by dotted lines. The arrows show some of the many possible radiative transitions.

tion and the kinetic-energy spectrum gives the branching ratios between various open photon channels.

IV. RESULTS AND DISCUSSION

In this work, our aim is to explore the dynamics of the multiphoton dissociation of the simplest polar molecule HD^+ under two fields of different frequencies which are varied within certain limits. The frequency of the first field, which we denote by ω_1, is varied between 10 000 and 10 100 cm^{-1}, keeping the frequency of the second field ω_2 constant. ω_2 is varied starting from 19 500 cm^{-1} and upto 21 522 cm^{-1}, which is the dissociation threshold of the HD^+ molecule from the initial $v_i=0,J_i=0$ level. The one-dimensional (1D) dynamics of this system was earlier investigated by our group [6]. Through the present 3D calculation, we want to explore both the branching ratios of photofragments and their angular distributions for various frequencies. In the absence of rotations, the values of the branching ratios cannot be reliable while the concept of angular distributions is, of course, meaningless for a rotationless model.

In Fig. 1, we show the potential-energy curves of the two lowest states of the free molecule, which have been considered in our calculation. In the diabatic representation, these states are denoted by GS and ES. The unperturbed initial level $v_i=0,J_i=0$ on the GS potential curve has been shown. Dissociation may occur by absorption of more than one photon of one or two frequencies but not by absorption of a single photon of either frequency. Simultaneous absorption

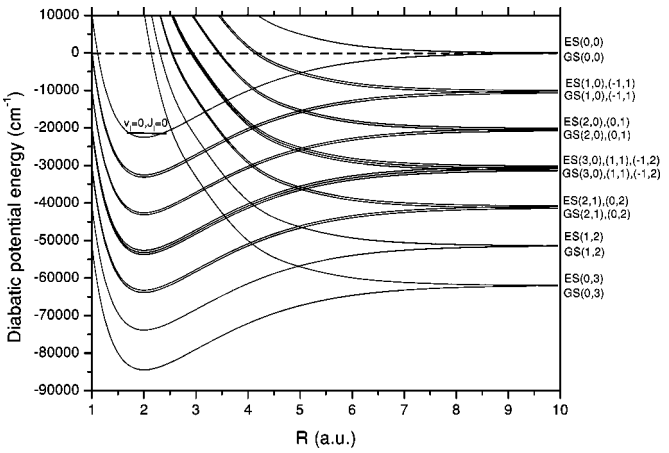

FIG. 2. Diabatic potential-energy curves for the two electronic states GS and ES of HD^+ at laser frequencies $\omega_1=10\,053$ cm^{-1} and $\omega_2=20\,668$ cm^{-1}. The unperturbed eigenenergy of the initial vibrational-rotational level $v_i=0,J_i=0$ is also indicated.

and emission of a number of photons of different frequencies can also occur. We have also shown the energy after the absorption of two photons of each frequency as well as the energy of the field-free $v=6,J=1$ level on the GS curve. The arrows indicate some of the possible transitions caused by absorption or stimulated emission.

A few diabatic (noninteracting field plus molecule) and field dressed adiabatic potential-energy curves of HD^+ for different numbers of absorbed photons are displayed in Figs. 2 and 3, respectively. The adiabatic curves have been drawn for intensity 1 TW/cm^2 of each field and for linear parallel polarizations of the fields. Both the diabatic and adiabatic curves are plotted for the fields of frequencies $\omega_1=10\,053$ cm^{-1} and $\omega_2=20\,668$ cm^{-1}. The numbers of photons of frequencies ω_1 and ω_2 absorbed are denoted by

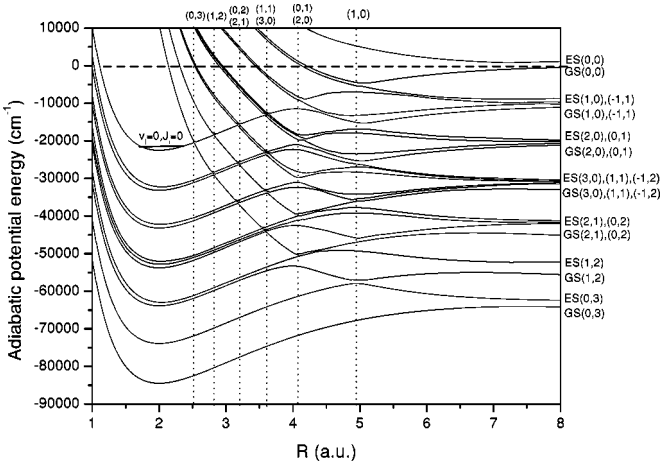

FIG. 3. Adiabatic potential-energy curves for the two electronic states GS and ES of HD^+ at laser frequencies $\omega_1=10\,053$ cm^{-1} and $\omega_2=20\,668$ cm^{-1}, and each laser intensity 1 TW/cm^2. The dressed energy corresponding to the initial field-free rovibrational level $v_i=0,J_i=0$ is also shown. The vertical dotted lines indicate the positions of avoided crossings due to multiphoton interactions involving different photon numbers (n_1,n_2).

(n_1,n_2) and each of the diabatic curves can be labeled by the three labels, GS or ES for the electronic state and (n_1,n_2). It is to be noted that the spreading of these curves due to molecular rotation has not been displayed. The adiabatic curves arise from field induced mixing of the diabatic curves and thus cannot be uniquely labeled. For simplicity, only one of the many diabatic and adiabatic curves with differing rotational properties has been plotted. We shall base our discussion on these simplified diagrams. In reality, for a 3D model each curve should have a band associated with it.

We note that the adiabatic curves arising from the diabatic curves GS and ES of the undressed field plus molecule system exhibit avoided crossings at various points. These crossing are the consequences of the multiphoton interactions between the corresponding diabatic curves. The number of photons involved at each crossing is denoted at the top of the figure in the notation (n_1,n_2). Because the energy of each combination of photon numbers is fixed, a multiphoton interaction involving a definite combination (n_1,n_2) takes place between the appropriate GS and ES diabatic potentials at a definite internuclear separation. For example, all avoided crossings between GS and ES near 2.5 a.u. arise due to the exchange of three ω_2 photons and so on. Since $\omega_2 \approx 2\omega_1$, the avoided crossing arising due to the exchange of n_1 photons of frequency ω_1 and n_2 photons of frequency ω_2 is degenerate with that due to the exchange of n_1+2n_2 photons of frequency ω_1.

These avoided crossings play an important role in the excitation and dissociation dynamics of the molecule. At each avoided crossing, depending on the strength of the interaction, the molecule can follow the adiabatic path or alternatively, the nonadiabatic interactions due to the nuclear motion may force the molecule to follow the nonadiabatic path. In other words, the resulting wave functions in the presence of laser fields will not be purely adiabatic but a linear superposition of different adiabatic wave functions.

Apart from this, there will be a direct coupling of all orders between two GS states due to the presence of the permanent dipole moment of HD^+. Thus a molecule in the vibrational-rotational ground level can absorb a photon of appropriate frequency and make a transition to another field dressed bound or quasibound level of another field dressed state with a dominant GS character (if such a level exists).

In 1D calculation [6], this situation gave rise to vibrational resonances where the dissociation linewidth was drastically enhanced. As ω_2 was varied keeping ω_1 fixed, the positions of the vibrational resonances changed due to the modification of the long-range part of the potential. The dressed adiabatic state, which corresponds to the absorption of one ω_1 photon near the equilibrium, could support a quasibound level at the initial molecular energy for certain values of ω_2 only. For intermediate value of ω_2 the linewidth became very small and the molecule became exceptionally stable against dissociation.

Something similar happens in our model also. Figure 4(a) gives a crude plot of the total dissociation linewidth [full width at half maximum(FWHM)] as a function of ω_1 for a fixed value of $\omega_2 = 20\,668$ cm^{-1}. The values of ω_1 used here are near the field-free transition energy between the $v_i = 0, J_i = 0$ and $v = 6, J = 1$ levels. The dissociation linewidth is clearly enhanced at two values of ω_1. At the higher peak for $\omega_1 = 10\,053$ cm^{-1} the enhancement is more than eight times the background. This, of course, suggests an intermediate one-photon vibrational resonance. However, due to the presence of the rotational degree of freedom, mixed rotational states are now formed, each consisting of a linear superposition of states with different rotational quantum numbers. A second resonance with such a mixed state which does not have a strong transition moment from the GS (0,0) state must be responsible for the resonant increase of the dissociation linewidth at the lower frequency of $10\,030$ cm^{-1}.

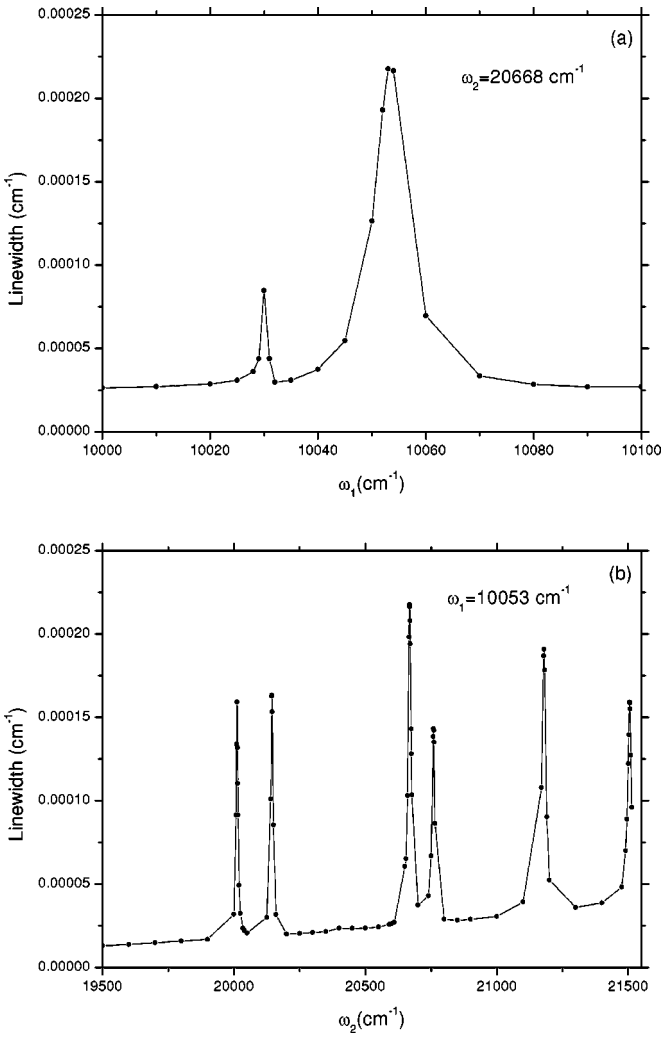

FIG. 4. The total dissociation linewidth of HD^+ from the initial level $v_i = 0, J_i = 0$ at each laser intensity 1 TW/cm^2. (a) ω_1 is varied and ω_2 is fixed at 20 668 cm^{-1}, (b) ω_2 is varied and ω_1 is fixed at 10 053 cm^{-1}.

Now, we keep ω_1 fixed at 10 053 cm^{-1} and plot the total dissociation linewidth (FWHM) as a function of ω_2. The plot is shown in Fig. 4(b). Again, for the fixed value of ω_1, we get resonance enhancements at different values of ω_2 which are five to seven times the background. The resonances are with the level which would be $v = 6, J = 1$ in the potential with the GS (1,0) character near the equilibrium in the absence of ω_2. The single-photon interaction between GS (1,0)

and ES (1,1) potentials causes a double-well adiabatic potential which has a GS (1,0) character near the equilibrium position. Of course, now there are several such potentials and a number of avoided crossings because of rotational spreading and this makes the picture very complicated. One of the consequences of this complication is that even midway between intermediate resonances, the destructive interference between contributions of closely spaced neighboring quasibound levels cannot efficiently stabilize the molecule. Zero linewidth is never obtained, for the many nonresonant paths through laser induced adiabatic states with a mixed rotational state character can never manage to cancel completely.

For this reason we tend to get only a few peaks between $\omega_2 = 19\,500$ and $21\,500$ cm^{-1}. Precisely, we get three groups of two peaks each. Visualization of what is happening here is rather difficult. However, the basic idea of the 1D model described in detail earlier [6] should remain valid. If we concentrate only on the single-photon interaction neglecting the multiphoton avoided crossings, then the adiabatic potential corresponding to GS (1,0), near the equilibrium, becomes double welled with the energy lying very near the asymptotic energy and the lower peak. The barrier height and the positions are sensitive to ω_2 and thus so are the energies of the possible bound levels. When we vary ω_2, a resonance occurs whenever the position of one of such bound level coincides with the initial energy of the field-free ground level. Because of the presence of many adiabatic states with a mixed rotational character, we obtain two peaks at closely spaced values of ω_2. These are the signatures of bound levels in two different adiabatic potentials within the band.

This is tested in Figs. 5(a) and 5(b) where we have plotted the total overlaps (T_i) of the free scattering wave function with two different bound level wave functions, the $v_i = 0, J_i = 0$ wave function in the diabatic state GS (0,0) and the $v = 6, J = 1$ wave function in the diabatic state GS (1,0) at $\omega_1 = 10\,053$ cm^{-1}. In Fig. 5(a), for $\omega_2 = 20\,668$ cm^{-1}, both the overlaps give a single line spread over a range of energy. The peaks of the two overlaps are exactly at the same energy. Different horizontal scales are used for the two overlaps in Fig. 5(a) in view of their very different widths. The width of the GS (0,0) overlap is 2.18×10^{-4} cm^{-1}, while the width of the overlap with the GS (1,0) ($v = 6, J = 1$) state is a few cm^{-1}. This shows that the laser shifted initial level acquires a distinct $v = 6, J = 1$ character in the GS (1,0) potential. This suggests that in the range of internuclear separation where there is no avoided crossing, the molecular wave function has a mixed character for this combination of frequencies. This mixed character must arise through the one-photon interaction mediated through the permanent dipole. There is no evidence of a two-photon interaction leading to a GS $(-1,1)$ character.

Figure 5(b) shows the same overlaps but for $\omega_2 = 20\,400$ cm^{-1} where there is no peak in the linewidth [Fig. 4(b)]. As earlier [Fig. 5(a)], here also different horizontal scales are used for the two overlaps in view of their different widths. In this case the overlap between the solution of the CC equation and the $v = 6, J = 1$ bound level wave function in the GS (1,0) potential is spread over a very wide range of energy without any single well-defined peak. In fact the

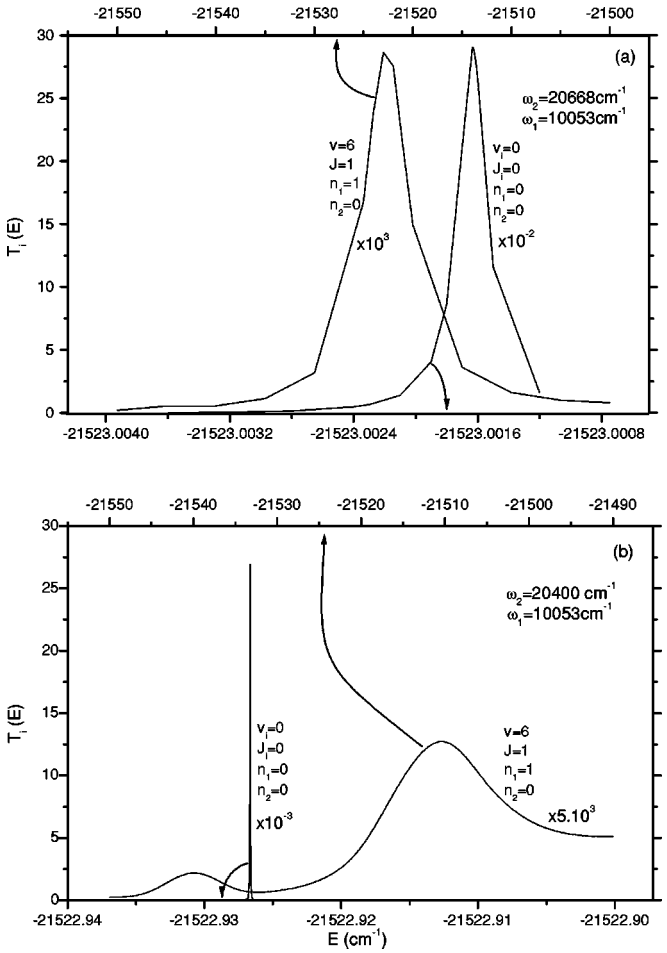

FIG. 5. Total overlaps T_i between the free scattering wave functions and the bound wave functions of HD^+ in the diabatic potentials GS (0,0) and GS (1,0) for $v_i = 0, J_i = 0$ and $v = 6, J = 1$, respectively, plotted as function of the total energy E at each laser intensity 1 TW/cm^2. (a) at resonance frequency $\omega_2 = 20\,668$ cm^{-1}, (b) at off-resonance frequency $\omega_2 = 20\,400$ cm^{-1}. $\omega_1 = 10\,053$ cm^{-1} in both the cases. The energy (E) scales corresponding to the curves are indicated by arrows.

overlap spreads over hundreds of cm^{-1}. Such diffuseness indicates that the $v = 6, J = 1$ level is not even transiently occupied at any stage of scattering. This implies that the resonant enhancement of linewidth occurs whenever a photon absorption occurs to the $v = 6, J = 1$ level of the diabatic potential GS (1,0), which adiabatically becomes quasibound on interaction with more photons.

Figure 6 shows the branching ratios of the photofragments to different photon absorption channels as function of ω_2 for ω_1 fixed at $10\,053$ cm^{-1}. We see that on resonance the ES (1,1) channel is the dominant one but at off-resonance the probability of dissociation through this channel is negligible. For the off-resonance dissociation the most effective channels are the ES (1,2), ES (2,1), and, to a lesser extent, GS (1,2). At the frequencies where resonance occurs, the contributions of all these channels reach minima. However, at the resonance frequencies there is a small contribution from the ES (3,0) channel.

These findings can be qualitatively understood by refer-

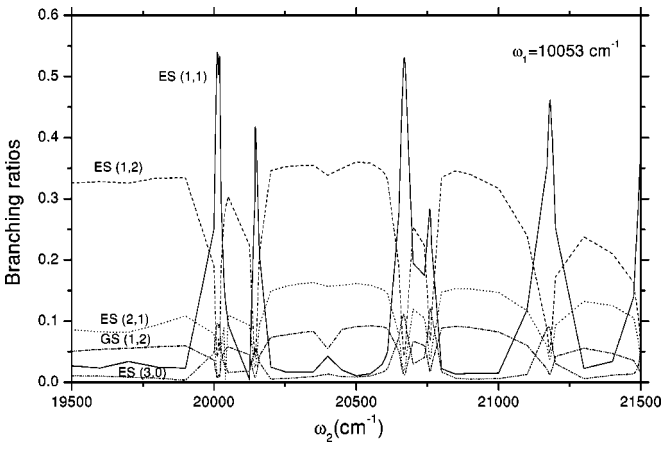

FIG. 6. The branching ratios of the photofragments of HD^+ to different absorption channels as functions of ω_2 keeping ω_1 fixed at 10 053 cm^{-1} at each laser intensity 1 TW/cm^2.

ring to Fig. 3 again. For the adiabatic potential curve corresponding, near equilibrium, to the diabatic potential GS (1,0), the most important avoided crossing will be around 4 a.u., since the wave function (which has the $v=6, J=1$ character) can be appreciable in this region. Dissociation can occur through further one ω_2 photon absorption at 4.1 a.u. and subsequent adiabatic passage with a further nonadiabatic transition near 5 a.u. It is clear from Fig. 2 that such paths would cause dissociation through ES (1,1) and ES (3,0) channels only. However, when this GS (1,0) potential plays no role in the process as an intermediate, most of the dissociation should occur through the (0,3) avoided crossing near 2.5 a.u., because the initial wave function is appreciable only in this region. In this case, after adiabatic passage through the (3,0) crossing, further higher-order multiphoton interaction may not play important roles as distinct from the one-photon transition near 4 and 5 a.u. It can be seen that a three-photon transition followed by diabatic passage and further single-photon transition should give the final states, which are observed to be most probable when there is no resonance with any GS state.

In effect, below threshold frequencies and for such comparatively low intensity, nonadiabatic paths will be preferred over adiabatic passage through higher-order crossings. Single-photon crossings occur at large internuclear separation, and at small internuclear separation single-photon transitions can take place only by a vibrational transition. However, vibrational levels are sensitive to the frequencies of both fields and such transitions can occur only for particular field combinations. In other cases, direct multiphoton transitions through higher-order avoided crossings are the only possibility if we start from a narrow localized wave function. However, the cross sections of such multiphoton transitions are much smaller compared to those occurring through resonant paths. The interesting effects occur because by changing ω_2 the field dressed energy of the $v=6, J=1$ level (for $n_1=1, n_2=0$) is changed and this particular level can act as an important long-lived intermediate state for certain values of ω_2 when ω_1 is kept fixed. This is demonstrated in Fig. 5 where it is clearly seen that the molecule can be said to exist in the $v=6$, $J=1$ level after a one-photon absorption only for certain values of the frequency ω_2 which we call resonance frequencies. It is worth emphasizing here that strong selectivity with respect to the photon number absorbed is obtained by varying the second frequency ω_2 in the presence of the first frequency ω_1. In our formulation, the final populations in the GS and ES states imply the formation of H^+ and D^+ ions, respectively. No further transformation is necessary to obtain the atomic states.

Previously, it has been shown that the branching ratio between the two states and between the various possible kinetic energies of the photofragments (resulting from the absorption of different number of photons) depends on the intensity and frequency when light of a single frequency is used [3]. It is also strongly dependent on the shape of the initial wave function. For example, if the wave function and the intensity are such that a tunneling or a bond softening transition is most dominant then the molecule should prefer to dissociate by the absorption of a single photon and it ends up in the ES state. Similarly, for comparatively weak fields, the dissociation from low vibrational levels by a three-photon absorption to the ES state may be made to dominate [3]. Charron *et al.* [5] obtained almost an equal flux in the two states GS and ES for 780 nm wavelength and from initial $v_i=3$ level of HD^+ for $I=10$ TW/cm^2. They argued that the dissociative energy flux does not "feel" the asymptotic energy splitting between the two states. Earlier, we obtained similar behavior for the above-threshold dissociation fluxes at several intensities depending on the initial wave function and the photon number channels and interpreted them as the outcome of competition between different adiabatic and diabatic pathways to dissociation [3]. The outcome of this competition depends on the

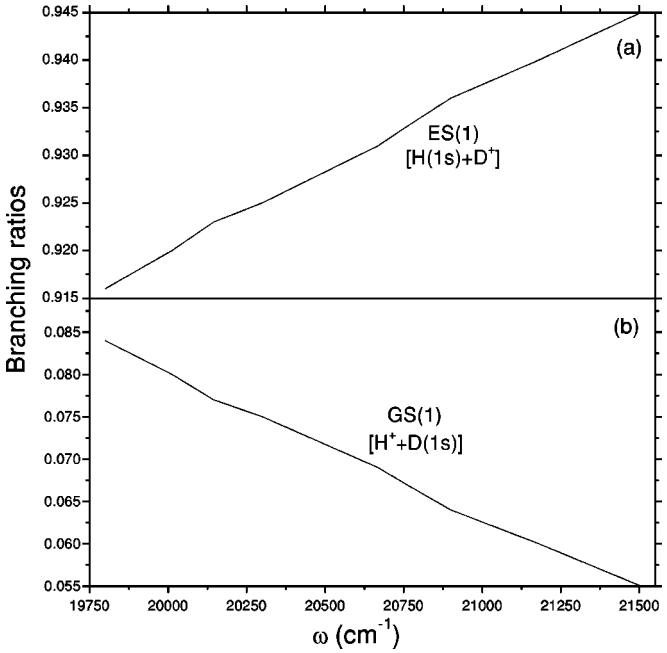

FIG. 7. The branching ratios of the photofragments of HD^+ for the initial level $v_i=6, J_i=0$ as functions of one-color laser frequency ω at laser intensity $I=1$ TW/cm^2. (a) for ES (1) $[H(1s)+D^+]$, (b) for GS (1) $[H^++D(1s)]$.

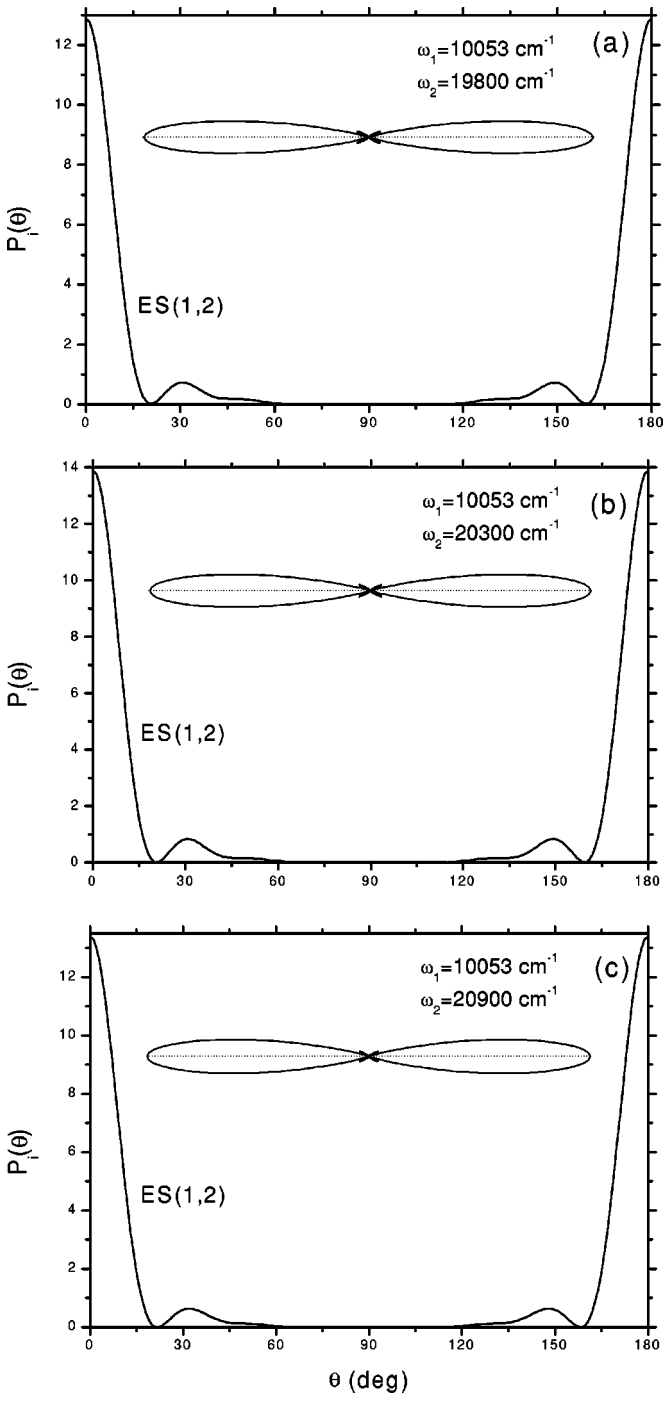

FIG. 8. Angular distributions, in both linear and polar plots, of the photofragments of HD^+ to (open) photon channel ES (1,2) for nonresonant frequencies ω_2 with ω_1 fixed at 10 053 cm^{-1} at each laser intensity 1 TW/cm^2. (a) $\omega_2 = 19\,800$ cm^{-1}, (b) $\omega_2 = 20\,300$ cm^{-1}, (c) $\omega_2 = 20\,900$ cm^{-1}.

frequency and intensity of the laser and also on the shape of the initial wave function.

In Fig. 7, we present the branching ratios for the fluxes in the two states GS and ES from the initial $v_i = 6, J_i = 0$ level of HD^+ in a single-frequency field. Almost at all the frequencies considered, the flux in the ES (1) channel is much preferred over that in the GS (1) channel. For high initial vibrational level and the intensity used by us, this should be the normal outcome. This is the general pattern expected for a process driven by lowering the adiabatic potential barrier. Very small fluxes to other photon absorption channels determined by higher-order avoided crossings are found to be equally distributed between the GS and ES states but the crossings are not effective when the initial level is $v_i = 6, J_i = 0$.

The different mechanisms of the multiphoton transitions in resonant and nonresonant cases result in very different angular distribution of the fragments in the two cases. Figures 8(a)–8(c) show the angular distribution patterns for three nonresonant frequencies ω_2 in the channel ES (1,2) where the flux is maximum. In each case, the angular distribution pattern follows the usual expected pattern of a narrow angular distribution in the forward and backward directions obtained earlier for the single-frequency multiphoton dissociation [7]. The half-width of the pattern is about 9°. The axis is along the polarization direction of the linearly polarized lasers (both polarized in the same direction). Thus we may say that the physics involved in the two-frequency non-

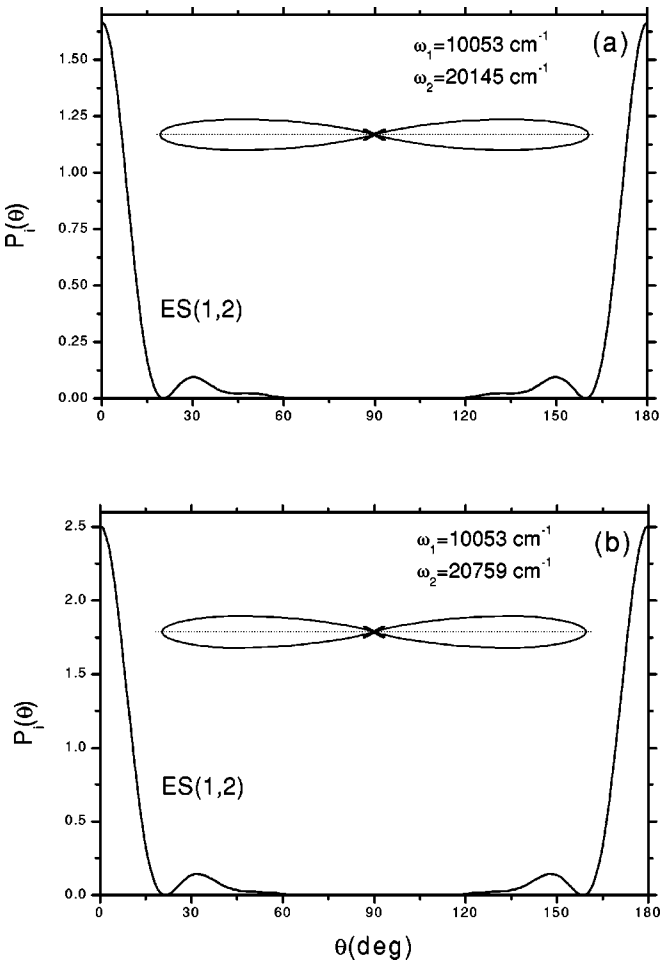

FIG. 9. Angular distributions, in both linear and polar plots, of the photofragments of HD^+ to (open) photon channel ES (1,2) for resonant frequencies ω_2 with ω_1 fixed at 10 053 cm^{-1} at each laser intensity 1 TW/cm^2. (a) $\omega_2 = 20\,145$ cm^{-1}, (b) $\omega_2 = 20\,759$ cm^{-1}.

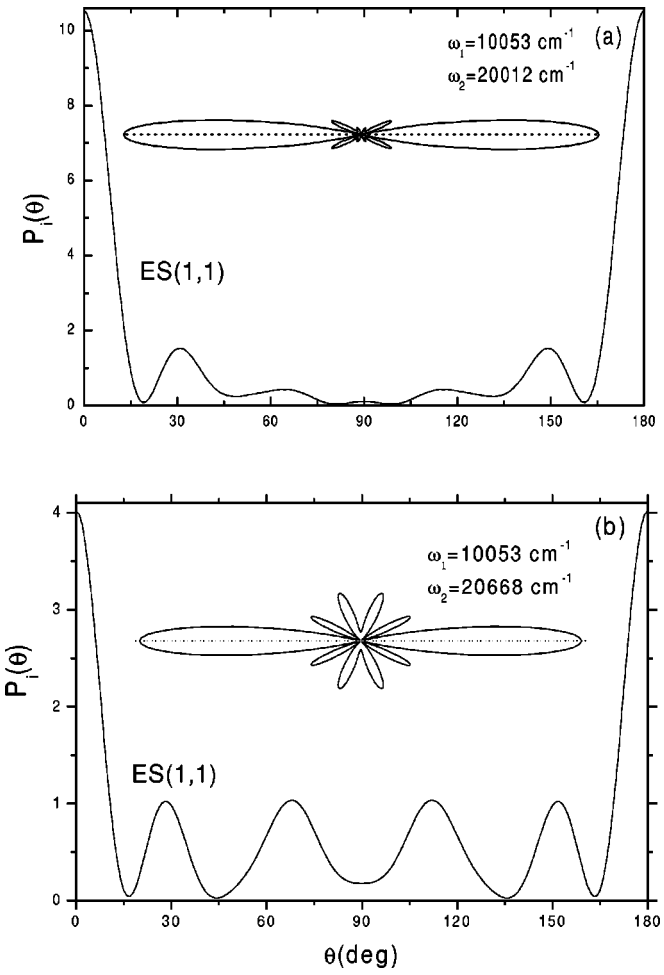

FIG. 10. Angular distributions, in both linear and polar plots, of the photofragments of HD^+ to the (open) photon channel ES (1,1) for resonant frequencies ω_2 with ω_1 fixed at 10 053 cm^{-1} at each laser intensity 1 TW/cm^2. (a) $\omega_2 = 20\,012$ cm^{-1}, (b) $\omega_2 = 20\,668$ cm^{-1}.

resonant multiphoton dissociation is the same as that for such single-frequency fragmentation.

In Figs. 9(a) and 9(b), the angular distribution in the ES (1,2) channel is plotted when ω_2 is resonant. This channel has a very small relative flux on resonance (Fig. 6) and the angular distribution pattern is almost the same as in the off-resonance case (Fig. 8).

Figures 10(a) and 10(b) plot the angular distribution in the ES (1,1) channel at frequencies ω_2 for which the resonant enhancement of the linewidth is obtained. These angular distributions of the fragments exhibit very different patterns. They all have a large number of scattering rings [15], which are peaks in the angular distributions at various intermediate angles. The rings become more and more prominent as ω_2 is increased. The spatial spread of the wave function before dissociation as well as the dense manifold of coupled rotational levels present at large internuclear separation may be responsible for such a behavior.

V. CONCLUSIONS

We have presented the time-independent CC calculation of the two-frequency intense-field multiphoton dissociation of HD^+. We address the problems of the multiphoton dissociation linewidth, branching ratios, and angular distributions of the photofragments of HD^+ induced by two strong linearly polarized parallel laser fields of equal intensity of 1 TW/cm^2. No reliable values of the branching ratios to different channels can be obtained unless rotational motion is taken into account. Angular spread of the fragments is, obviously, a consequence of the rotational motion. Both the branching ratios and the angular distributions show striking changes when the frequency of one of the lasers is changed. We show that at some combinations of the frequencies, an intermediate one-photon vibration-rotation resonance takes place due to the presence of the permanent dipole moment of HD^+. This intermediate resonance is responsible for the drastic changes observed. The branching-ratio pattern can be explained by invoking the dynamics on a simplified set of adiabatic potentials obtained due to the modification of the field plus molecule potentials by the field plus molecule interaction. However, for an explanation of the scattering rings on resonance, a detailed analysis of the dynamics of the angular motion on a large number of rotationally coupled adiabatic surfaces may have to be made.

[1] A. Giusti-Suzor, X. He, O. Atabek, and F.H. Mies, Phys. Rev. Lett. **64**, 515 (1990).
[2] A. Giusti-Suzor, F.H. Mies, L.F. DiMauro, E. Charron, and B. Yang, J. Phys. B **28**, 309 (1995).
[3] A. Datta, S. Saha, and S.S. Bhattacharyya, J. Phys. B **30**, 5737 (1997), and references cited therein.
[4] E. Charron, A. Giusti-Suzor, and F.H. Mies, Phys. Rev. Lett. **75**, 2815 (1995).
[5] E. Charron, A. Giusti-Suzor, and F.H. Mies, J. Chem. Phys. **103**, 7359 (1995).
[6] A. Datta and S.S. Bhattacharyya, Phys. Rev. A **59**, 4502 (1999).
[7] S. Sen, S. Ghosh, S.S. Bhattacharyya, and S. Saha, J. Chem. Phys. **116**, 1286 (2002).
[8] F.H. Mies and A. Giusti-Suzor, Phys. Rev. A **44**, 7547 (1991).
[9] G.G. Balint-Kurti and M. Shapiro, Adv. Chem. Phys. **60**, 403 (1985).
[10] R.E. Moss and I.A. Sadler, Mol. Phys. **61**, 905 (1987).
[11] A. Carrington and R.A. Kennedy, Mol. Phys. **56**, 935 (1985).
[12] D.R. Bates, J. Chem. Phys. **19**, 1122 (1951).
[13] S. Ghosh, M.K. Chakrabarti, S.S. Bhattacharyya, and S. Saha, J. Phys. B **28**, 1803 (1995).
[14] F. H. Mies (private communication).
[15] L.F. DiMauro and P. Agostini, Adv. At., Mol., Opt. Phys. **35**, 79 (1995).